

Quantitative Evaluation of Silicon Displacement Induced by Arsenic Implantation Using Silicon Isotope Superlattices

Yasuo Shimizu, Masashi Uematsu, Kohei M. Itoh*, Akio Takano¹, Kentarou Sawano², and Yasuhiro Shiraki²

Department of Applied Physics and Physico-Informatics, Keio University, 3-14-1 Hiyoshi, Kohoku-ku, Yokohama 223-8522, Japan

¹NTT Advanced Technology Corporation, 3-1 Morinosato-Wakamiya, Atsugi, Kanagawa 243-0124, Japan

²Research Center for Silicon Nano-Science, Advanced Research Laboratories, Musashi Institute of Technology, 8-15-1 Todoroki, Setagaya-ku, Tokyo 158-0082, Japan

Received November 21, 2007; accepted December 28, 2007; published online January 25, 2008

We established a new method for evaluating quantitatively the silicon atomic displacement as a function of the depth from the surface induced by arsenic implantation into a silicon wafer. A simulation based on a convolution integral was developed successfully to reproduce the experimental depth profiles of isotopes in the arsenic-implanted ²⁸Si/³⁰Si isotope superlattices, from which the average distance of the silicon displacements due to the collisions with implanted arsenic is obtained. We show that it takes the average displacement of ~ 0.5 nm to make the structure appear amorphous by transmission electron microscopy. © 2008 The Japan Society of Applied Physics

DOI: 10.1143/APEX.1.021401

Arsenic (As) implantation, which is widely used for the formation of shallow junctions in silicon (Si) nano-transistors, induces radiation damages that can significantly affect the redistribution of dopants during post-implantation annealing. Therefore, the relation between the distribution of implanted As and damage in crystalline Si has been studied extensively.^{1–7} While the depth profiles of As impurities are routinely measured by secondary ion mass spectrometry (SIMS),⁸ a quantitative method to directly evaluate the average distance of the Si atomic displacements associated with the implantation does not exist. The ion-channeling and cross-sectional transmission electron microscopy (XTEM) can only estimate the fraction of the Si atoms displaced from the substitutional sites in the single-crystalline region.² Such evaluation becomes almost hopeless in the amorphous region induced by the implantation. The present letter reports a method to evaluate the average distance of the Si displacements as a function of the depth from the implanted surface both in the amorphous and single-crystalline regions. Our statistical analysis of the perturbed Si isotope profiles measured by SIMS allows determination of the displacement with the accuracy < 1 nm, which is significantly better than the direct determination by SIMS. We find that the Si displacements vary significantly even within the region that appears “uniformly amorphous” by XTEM. The critical displacement (σ_c), which we define as the displacement at the interface of the single crystalline and amorphous regions observed by XTEM, is ~ 0.5 nm.

A ²⁸Si(2.7 nm)/³⁰Si(2.7 nm) isotope superlattice was grown by solid-source molecular beam epitaxy.^{9,10} A high resistivity ($\rho > 2000 \Omega\text{-cm}$), 2-inch, *n*-type, {001}-oriented Fz ^{nat}Si (²⁸Si: 92.2%, ²⁹Si: 4.7%, ³⁰Si: 3.1%) wafer was employed as a substrate. A ^{nat}Si buffer layer of ~ 100 -nm-thick was formed prior to the growth of the isotope superlattice that is composed of the alternating layers of isotopically pure ²⁸Si (99.92%) and ³⁰Si (99.3%). ⁷⁵As⁺ ions were implanted at room temperature into the superlattice with the energy of 25 keV corresponding to the projected range of ~ 20 nm, and with the doses of 1×10^{13} or $1 \times 10^{15} \text{ cm}^{-2}$ at a tilt angle of 7° . The depth profiles of Si isotopes and As were obtained by SIMS (ATOMIKA SIMS-4000), using the Cs⁺ primary ion beam at an energy of 1 keV with

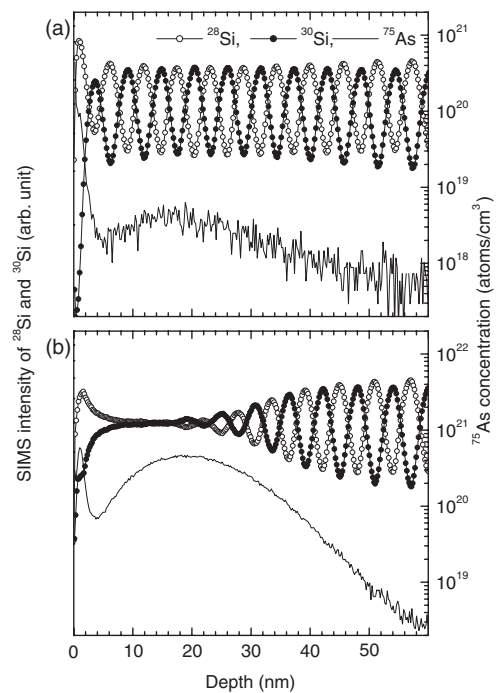


Fig. 1. Depth profiles of ²⁸Si (open circles), ³⁰Si (filled circles), and ⁷⁵As (solid curve) measured by SIMS in the ²⁸Si(2.7 nm)/³⁰Si(2.7 nm) isotope superlattices after ⁷⁵As⁺ implantation at the energy of 25 keV with the doses of (a) $1 \times 10^{13} \text{ cm}^{-2}$ and (b) $1 \times 10^{15} \text{ cm}^{-2}$.

the 45° incident angle. The sputtering rate was assumed to be constant. XTEM observations were performed with a TECNAI F12 electron microscope operating at 200 kV.

Figure 1(a) shows the depth profiles of ²⁸Si, ³⁰Si, and ⁷⁵As in the Si isotope superlattice implanted with As using the energy of 25 keV and dose of $1 \times 10^{13} \text{ cm}^{-2}$. With such a low dose, the alternating depth profiles of ²⁸Si and ³⁰Si are almost unperturbed even after the implantation in comparison with the profiles of ²⁸Si and ³⁰Si before the implantation [Fig. 2(a)]. Note that the actual interfaces between ²⁸Si and ³⁰Si layers are abrupt (the degree of intermixing is only two atomic layers)^{9,10} and the smearing of the ²⁸Si and ³⁰Si profiles is due to the so-called SIMS artifact (knock-on mixing, etc.). On the other hand, as shown in Fig. 1(b), the same energy but a factor of one hundred times higher dose of implantation of $1 \times 10^{15} \text{ cm}^{-2}$ leads to perturbation of

*E-mail address: kitoh@appi.keio.ac.jp

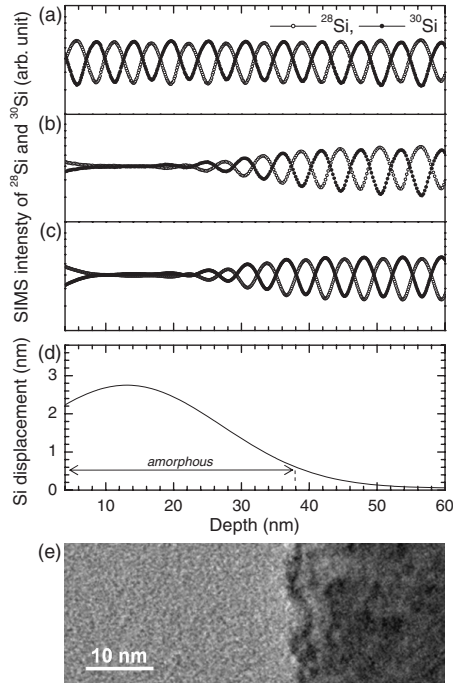


Fig. 2. Depth profiles measured by SIMS of ^{28}Si (open circles) and ^{30}Si (filled circles) in the Si isotope superlattices (a) before implantation and (b) after implantation with the energy of 25 keV and the dose of $1 \times 10^{15} \text{ cm}^{-2}$. (c) Simulated profiles using the convolution integral model described in the text. (d) The depth dependence of the displacement $\sigma(x)$ of the Si atoms induced by the As implantation. (e) XTEM image of the sample implanted with the same condition with the depth scale same as (a)–(d).

the ^{28}Si and ^{30}Si periodic profiles all the way to a depth of $\sim 50 \text{ nm}$. The following simulation based on a convolution integral is employed to reproduce the perturbed depth profile of ^{28}Si and ^{30}Si to obtain quantitatively the characteristic length of Si displacements as a function of the depth (x) from the implanted surface.

$$C_{\text{aft-imp}}(x) = \int C_{\text{bef-imp}}(x')g(x-x')dx'. \quad (1)$$

Here $C_{\text{bef-imp}}(x)$ and $C_{\text{aft-imp}}(x)$ represent the concentrations of ^{28}Si and ^{30}Si in the Si isotope superlattice before and after implantations, respectively. $g(x)$ is a Gaussian function:

$$g(x) = \frac{1}{\sqrt{2\pi}\sigma} \exp\left(-\frac{x^2}{2\sigma^2}\right). \quad (2)$$

$\sigma(x)$ is the distance of the displacement as a function of the depth x :

$$\sigma(x) = k \exp[-(x-c)^2/(2d^2)], \quad (3)$$

where k , c , and d are the parameters of peak amplitude, peak position, and peak width, respectively. It is known that the distribution of the displacement of atoms in solids by ion implantation can be approximated by Gaussian except for the tails.¹¹⁾ The values of k , c , and d are determined by direct comparison with the experimentally obtained depth profiles of the implanted sample.

Figure 2(a) shows the depth profiles of ^{28}Si and ^{30}Si in the Si isotope superlattice before implantation measured by SIMS. Figure 2(b) shows the depth profiles in the implanted

sample [the same ones as shown in Fig. 1(b)]. We simulated the profiles in Fig. 2(b) in the following manner. First, we reproduce the profiles of the as-grown sample that initially has rectangular isotopic profiles [Fig. 2(a)] using the mixing roughness information-depth (MRI) model.¹²⁾ This model includes atomic mixing (w) and surface roughness (s) for the theoretical description of the depth resolution function for SIMS profiles. The change of the concentration C with sputtered depth x is given by

$$\frac{dC(x)}{dx} = \frac{C^0(x+w) - C(x)}{w}, \quad (4)$$

where $C^0(x+w)$ is the original unaltered concentration of C at a distance w in front of instantaneous surface at x . The roughness is taken into account by superposition of a normalized Gaussian broadening as described by

$$C(x) = \frac{1}{\sqrt{2\pi}s} \int_{x-3s}^{x+3s} C^0(x') \cdot \exp\left[-\frac{(x-x')^2}{2s^2}\right] dx' \quad (5)$$

with the standard deviation of s . From this analysis, we obtained $w = 2.5 \text{ nm}$ and $s = 0.7 \text{ nm}$ to correct for the SIMS artifact. These parameters (w and s) are used to simulate the SIMS profiles after ion implantation [Fig. 2(b)], as mentioned below. Next, the convolution integral [eqs. (1)–(3)] is applied to the rectangular isotopic profiles, and then, the convoluted profiles are broadened using the MRI parameters obtained above to reproduce the profiles in Fig. 2(b). We choose the appropriate set of values $k = 2.7 \text{ nm}$, $c = 13 \text{ nm}$, and $d = 14 \text{ nm}$ in eq. (3) so that the convoluted and broadened profiles are comparable to the SIMS profiles after implantation. This allows us to plot the distribution of the Si displacement $\sigma(x)$ as shown in Fig. 2(d). The maximum displacement of 2.7 nm was induced by the implantation at 13 nm from the surface, which is shallower than 19 nm where the implanted As concentration becomes maximum as shown in Fig. 1(b). Figure 2(e) shows the XTEM image of the same implanted sample with the depth scale being the same as Figs. 2(a)–2(d). Due to the implantation, amorphization occurred between the surface and $\sim 38 \text{ nm}$ in depth, while the deeper region ($x > 38 \text{ nm}$) remained single-crystalline. Note that the periodicity of ^{28}Si and ^{30}Si remains even in the amorphous layer at $x = 20\text{--}38 \text{ nm}$. We define σ_c as the critical displacement occurring at the interface of the amorphous and single-crystalline regions in Fig. 2(e). This occurs at $x \sim 38 \text{ nm}$ with the value $\sigma_c \sim 0.5 \text{ nm}$, i.e., a displacement of approximately three times the Si–Si bond length. The $\sigma(x) > 0.5 \text{ nm}$ region appears “amorphous” by XTEM. However, even within the region $x < 38 \text{ nm}$ that appears “uniformly amorphous” by XTEM, the displacement varies significantly as shown in Fig. 2(d). Thus, $\sigma(x)$ provides the quantitative estimation of the degree of disorder in the implanted region.

To show the coherency of the analysis and significance of our finding, Fig. 3 shows the same analysis performed with two different implantation conditions.¹³⁾ The solid curve in Fig. 3(b) shows the Si displacement determined by using $k = 0.56 \text{ nm}$, $c = 13 \text{ nm}$, and $d = 14 \text{ nm}$ to reproduce the experimental data in Fig. 3(a). The XTEM in Fig. 3(c) shows two crystalline regions, near surface (0–3 nm) and deeper than 24 nm regions, and the amorphous region is sandwiched in between (3–24 nm). The displacement at

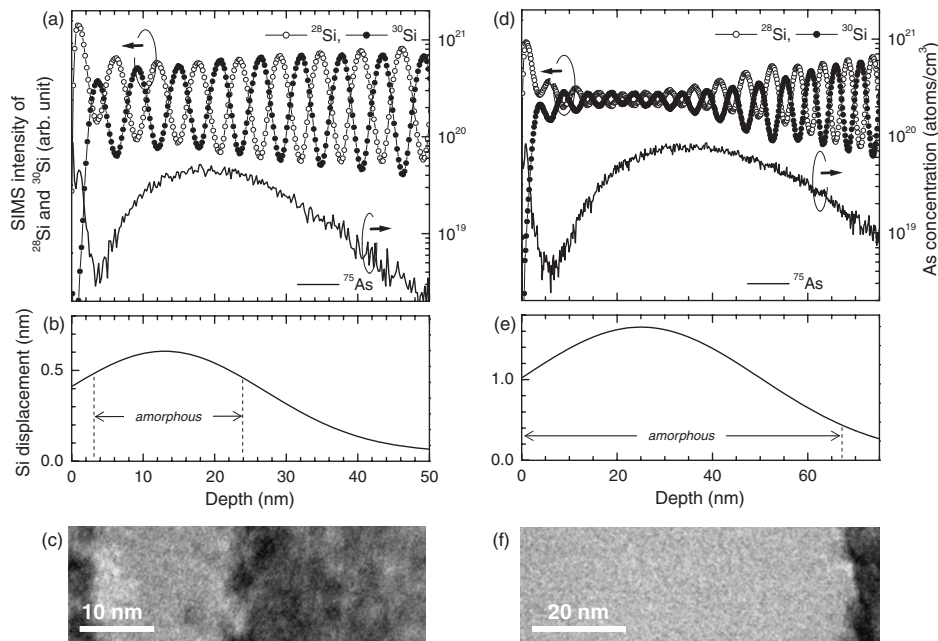


Fig. 3. (a) Depth profiles measured by SIMS of ^{28}Si (open circles) and ^{30}Si (filled circles) in the Si isotope superlattices after implantation with the energy of 25 keV and the dose of $1 \times 10^{14} \text{ cm}^{-2}$, (b) the depth dependence of the displacement $\sigma(x)$ of the Si atoms induced by the implantation, and (c) XTEM image. The same set of figures for the implantation energy of 60 keV and the dose of $3 \times 10^{14} \text{ cm}^{-2}$ is shown in (d)–(f).

the depths of 3 and 24 nm where the transition between crystalline and amorphous occurs, coincides exactly with the critical displacement 0.5 nm found in Fig. 2(d). The structure becomes amorphous (as determined by XTEM) only when the displacement exceeds the critical length of 0.5 nm. This also holds in another condition shown in Figs. 3(d)–3(f), where As ions are implanted at higher energy, 60 keV, making the structure amorphous from the surface all the way to ~ 70 nm. We obtained $k = 1.6 \text{ nm}$, $c = 25 \text{ nm}$, $d = 25 \text{ nm}$, and the displacement at ~ 70 nm shown in Fig. 3(e) is 0.5 nm.

In summary, we demonstrated the direct observation of the Si atomic displacement induced by As implantation using Si isotope superlattices. A simulation based on the convolution integral was developed successfully to reproduce the experimental SIMS depth profiles of Si isotopes in the As-implanted sample. We showed that it takes the average displacement of ~ 0.5 nm to make the structure appear amorphous by XTEM. Incorporation of $\sigma(x)$ into the next generation complementary metal oxide semiconductor process simulator may prove to be useful for the improvement of the simulation reliability.

Acknowledgment We acknowledge Professor E. E. Haller for fruitful discussions, Dr. T. Okui and H. Oshikawa for the technical support. This work has been supported in part by the Research Program on Collaborative Development of Innovative Seeds by Japan Science and Technology

Agency, the Special Coordination Funds for Promoting Science and Technology for Institute for Nano Quantum Information Electronics, and a Grant-in-Aid for the Global Center of Excellence for High-Level Global Cooperation for Leading-Edge Platform on Access Spaces from the Ministry of Education, Culture, Sports, Science, and Technology, Japan.

- 1) C. Tsamis, D. Skarlatos, G. BenAssayag, A. Claverie, W. Lerch, and V. Valamontes: *Appl. Phys. Lett.* **87** (2005) 201903.
- 2) G. Lulli, M. Bianconi, A. Parisini, S. Sama, and M. Servidori: *J. Appl. Phys.* **88** (2000) 3993.
- 3) G. Lulli, E. Albertazzi, M. Bianconi, R. Nipoti, M. Cervera, A. Carnera, and C. Cellini: *J. Appl. Phys.* **82** (1997) 5958.
- 4) M.-S. Son and H.-J. Hwang: *J. Vac. Sci. Technol. B* **18** (2000) 595.
- 5) L. Capello, T. H. Metzger, M. Werner, J. A. van den Berg, M. Servidori, L. Ottaviano, C. Bongiorno, G. Mannino, T. Feudel, M. Herden, and V. Holý: *J. Appl. Phys.* **100** (2006) 103533.
- 6) M. Posselt, B. Schmidt, T. Feudel, and N. Strecker: *Mater. Sci. Eng. B* **71** (2000) 128.
- 7) H. Oh, T. Sakaguchi, T. Fukushima, and M. Koyanagi: *Jpn. J. Appl. Phys.* **45** (2006) 2965.
- 8) J. B. Clegg: *Surf. Interface Anal.* **10** (1987) 332.
- 9) T. Kojima, R. Nebashi, K. M. Itoh, and Y. Shiraki: *Appl. Phys. Lett.* **83** (2003) 2318.
- 10) Y. Shimizu and K. M. Itoh: *Thin Solid Films* **508** (2006) 160.
- 11) D. K. Brice: *J. Appl. Phys.* **46** (1975) 3385.
- 12) S. Hofmann: *Surf. Interface Anal.* **21** (1994) 673.
- 13) Y. Shimizu, A. Takano, M. Uematsu, and K. M. Itoh: *Physica B* **401–402** (2007) 597.